

FULLY IMPLICIT IMPLEMENTATION OF BOUNDARY CONDITIONS IN OPERATOR-SPLITTING METHODS FOR STEADY INCOMPRESSIBLE NAVIER-STOKES EQUATIONS *

C. I. CHRISTOV[†], R. S. MARINOVA[‡], AND T.T. MARINOV[§]

Abstract. The steady incompressible Navier-Stokes equations in primitive variables are solved by means of an implicit vectorial operator-splitting scheme. The method allows for complete implicit coupling of the boundary conditions. Conservative approximations for the advective terms are employed on non-uniform staggered grid. The performance of the scheme is demonstrated on the lid-driven flow in a rectangular cavity of aspect ratio two. Results are obtained up to $Re = 5000$.

Key words. Navier-Stokes, Incompressible Viscous Flow, Operator-Splitting.

Introduction. In the incompressible Navier-Stokes equations the pressure is an implicit function for which no boundary conditions can be specified at the boundaries save the free surfaces. At the internal boundaries, the velocity components are prescribed (non-slip conditions): $\mathbf{u}|_{\partial\Omega} = \mathbf{u}_b$. The problem persists when vorticity function is used and no boundary conditions for the vorticity are available for the latter. This makes most of the algorithms subject to inextricable explicit element introduced by the iterative decoupling of the system. This is especially hard difficulty in operator-splitting schemes.

In the present work we consider the operator splitting for the incompressible Navier-Stokes equations. We propose a special treatment for the split operators which leave the pressure function coupled to one of the velocity components. Thus no artificial boundary conditions are needed for the pressure and the scheme is fully implicit.

In order not to obscure the main mathematical idea of the present paper we consider square domains with Cartesian coordinates. The geometric limitations for the proposed technique are just the same as for any other finite-difference method and after the numerical correctness is demonstrated the technique will be applied to more complex flow geometry and/or rheology. On this stage there are mathematical issues to be clarified which justifies the usage of a simple flow geometry. The second criterion in selecting the featuring example is the presence of benchmark calculations in the literature which can be used to test the novel technique.

Two analytic solutions in a square domain are considered as featuring examples, as well as the flow in rectangular lid-driven cavity of aspect ratio two. The numerical results obtained here are in very good quantitative agreement with the analytic solutions and with the numerical solutions from the literature for the available values of Reynolds number. For the cavity flow the Reynolds numbers for which the solution is obtained significantly exceed the range from the literature. This can be attributed to the strongly implicit nature of the algorithm proposed in the present work.

1. Formulation of the Problem. Consider the steady incompressible Navier-Stokes equations in closed domain $\mathbf{x} \in \Omega$, with piece-wise smooth boundary $\partial\Omega$

$$\frac{1}{Re} \Delta \mathbf{u} - \nabla p - \mathbf{C}[\mathbf{u}] = 0, \tag{1.1}$$

coupled by the continuity equation

$$\nabla \cdot \mathbf{u} = 0, \tag{1.2}$$

Here $\mathbf{u} = \mathbf{u}(\mathbf{x})$ is the velocity vector, $p = p(\mathbf{x})$ – the pressure. The Reynolds number is defined as $Re = UL/\nu$, where U is the characteristic velocity, L – characteristic length, ν – kinematic coefficient

*The work of C.I.C. is supported in part by Grant LEQSF(1999-2002)-RD-A-49 from the Louisiana Board of Regents. The support for T.T.M. from the Japan Society for the Promotion of Science (JSPS) under Grant No P99745 is gratefully acknowledged.

[†]Dept. of Mathematics, University of Louisiana at Lafayette, Lafayette, LA 70504-1010, USA

[‡]Dept. of Mathematics, Free University of Varna, Varna 9007, Bulgaria

[§]Dept. of Electr. Engineering, Saitama Institute of Technology, 1690, Fusaiji, Okabe, Saitama 369-0293, Japan

of viscosity. The operator $\mathbf{C}[\mathbf{u}]$ is a short-hand notation for the advective term. For this term we use the skew-symmetric form

$$\mathbf{C}[\mathbf{u}] = \nabla \cdot (\mathbf{u}\mathbf{u}) - \frac{1}{2}\mathbf{u}(\nabla \cdot \mathbf{u}), \quad (1.3)$$

which follows from the continuity equation (1.2) [16].

In lieu of the continuity equation the well-known ‘‘Poisson equation for pressure’’ can be used. Following [6] we use a modified version of this equation which is obtained after subtracting the continuity equation (1.2), namely

$$\frac{1}{\text{Re}}\Delta p - \nabla \cdot \mathbf{u} + \frac{1}{\text{Re}}\nabla \cdot \mathbf{C}[\mathbf{u}] = 0. \quad (1.4)$$

The advantages of the form (1.4) for pressure equation are discussed later.

The formulation with equation for pressure is equivalent to the original system only if the continuity equation (1.2) is satisfied also on the boundary (see, [13, 14])

$$\nabla \cdot \mathbf{u}|_{\partial\Omega} = 0. \quad (1.5)$$

For the above introduced ‘‘modified Poisson equation for the pressure, the justification can be found in [7, 6]).

To operator-splitting method can be used only for evolutionary systems, hence one needs to add in the governing system derivatives with respect to a time-like variable. For the $\psi - \omega$ formulation this has been done in [15] and called ‘‘Method of False Transients’’. In our case it amounts to adding in each equation of the governing system (1.1), (1.4), derivatives with respect to a *fictitious* time t . Upon convergence, the time-derivative term vanishes, and equations (1.1) and (1.4) are satisfied.

We recast the system for \mathbf{u} and p as the following vectorial system

$$\frac{\partial\boldsymbol{\theta}}{\partial t} = L[\boldsymbol{\theta}] + N[\boldsymbol{\theta}] + F[\boldsymbol{\theta}], \quad (1.6)$$

where

$$\boldsymbol{\theta} = \begin{pmatrix} u \\ v \\ p \end{pmatrix}, \quad L = \begin{pmatrix} \frac{1}{\text{Re}}\Delta & -\nabla & 0 \\ 0 & \frac{1}{\text{Re}}\Delta & -\nabla \\ -\nabla & -\nabla & \frac{1}{\text{Re}}\Delta \end{pmatrix}, \quad N = - \begin{pmatrix} C_u & 0 & 0 \\ 0 & C_v & 0 \\ 0 & 0 & 0 \end{pmatrix}, \quad F[\boldsymbol{\theta}] = \begin{pmatrix} 0 \\ 0 \\ \frac{1}{\text{Re}}\nabla \cdot \mathbf{C}[\mathbf{u}] \end{pmatrix}.$$

For incompressible flows, the pressure is defined up to an arbitrary function of time. For the sake of convenience we define this function similarly to [2, 1] as the average of the pressure at the specific time stage. To this end, the condition

$$\int_{\Omega} p(\mathbf{x}, t) \, d\mathbf{x} = 0, \quad \mathbf{x} \in \Omega, \quad (1.7)$$

is added as an additional constraint on the pressure function for each t .

Upon acknowledging the boundary conditions, we get for the evolution of the energy

$$\frac{d\mathcal{E}}{dt} = -\frac{1}{\text{Re}} \int_{\Omega} (\nabla\boldsymbol{\theta})^2 \, d\mathbf{x} + \frac{1}{\text{Re}} \int_{\Omega} p (\nabla \cdot \mathbf{C}[\mathbf{u}]) \, d\mathbf{x}. \quad (1.8)$$

Without the term we added in the Poisson equation for pressure, a non-definite term of unit order appears it in the right-hand side of equality (1.8) which term is not necessarily small on the initial stages of the iterative process. Now the only non-definite term is of order $O(\text{Re}^{-1})$.

2. Vectorial Operator-Splitting. Each iteration (time step) is implemented via operator splitting because of its computational efficiency. We employ the second Douglas scheme (see [10]) which is sometimes called ‘‘stabilizing correction’’. It is of first order in time, but has advantages for non-commuting operators (see [17]).

The two steps of the scheme of stabilizing correction read

$$\frac{\boldsymbol{\theta}^{n+1/2} - \boldsymbol{\theta}^n}{\tau} = A_1\boldsymbol{\theta}^{n+1/2} + A_2\boldsymbol{\theta}^n + G^n, \quad \frac{\boldsymbol{\theta}^{n+1} - \boldsymbol{\theta}^{n+1/2}}{\tau} = A_2(\boldsymbol{\theta}^{n+1} - \boldsymbol{\theta}^n), \quad (2.1)$$

τ is the increment of the fictitious time. Respectively, A_1 and A_2 are the x - and y - components of the operator $L + N$ form (1.6).

The implementation of the scheme of stabilizing correction corresponds to determining $\theta^{n+1/2}$ and θ^{n+1} from the equations

$$(I - \tau A_1)\theta^{n+1/2} = (I + \tau A_2)\theta^n + \tau G^n, \quad (I - \tau A_2)\theta^{n+1} = \theta^{n+1/2} - \tau A_2\theta^n, \quad (2.2)$$

$I \stackrel{\text{def}}{=} \begin{pmatrix} E & 0 & 0 \\ 0 & E & 0 \\ 0 & 0 & E \end{pmatrix}$, where E is the unitary operator. The notation (2.2) indicates that the solution can be found by inverting the one-dimensional grid operator first with respect to one variable and then with respect to the other variable. The half-time-step variable $\tilde{\theta}^{n+1/2}$ can be eliminated from (2.2) to get

$$(I + \tau^2 A_1 A_2) \frac{\theta^{n+1} - \theta^n}{\tau} = (A_1 + A_2)\theta^{n+1} + G^n. \quad (2.3)$$

It is readily seen now that upon convergence (i.e. when $\|\theta^{n+1} - \theta^n\| \rightarrow 0$), the solution of the evolution problem approaches a steady-state which does not depend on τ .

3. Difference Scheme. We use non-uniform grid (see Figure 3.1-a) which is staggered for u in x -direction and for v – in y -direction (see, also [4]). This allows one to use for the derivatives central differences with second-order of approximation on two-point stencils. The number of main grid lines (the p -grid) are respectively N_x and N_y . The numbers of intervals are $N_x - 1$ and $N_y - 1$. The coordinates of the grid points are (x_i, y_j) for $i = 1, \dots, N_x, j = 1, \dots, N_y$. The spacings of the p -grid are given by $h_i = x_{i+1} - x_i$, and $k_j = y_{j+1} - y_j$. The spacings for the u -grid and v -grid are as follows

$$h_1^u = h_1, \quad h_i^u = \frac{1}{2}(h_i + h_{i-1}) \text{ for } i = 2, \dots, N_x - 1, \text{ and } h_{N_x}^u = h_{N_x - 1},$$

$$k_1^v = k_1, \quad k_j^v = \frac{1}{2}(k_j + k_{j-1}) \text{ for } j = 2, \dots, N_y - 1, \text{ and } k_{N_y}^v = k_{N_y - 1}.$$

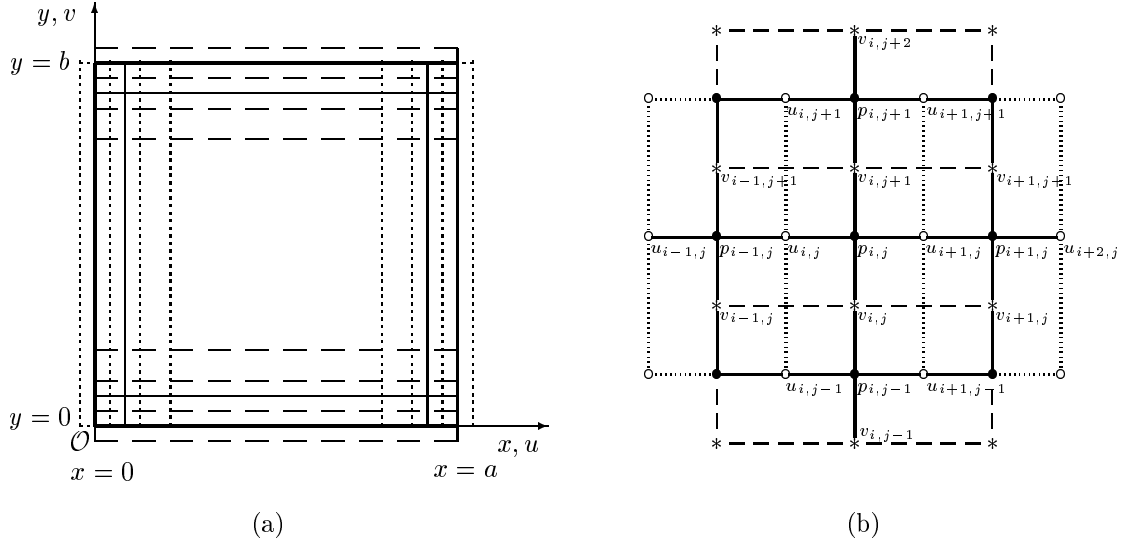


FIG. 3.1. Computational domain with the grid (a); the finite-difference stencil (b).

In Figure 3.1-b the pressure is sampled at the points labeled by “•”; function u – at “o”; function v – at “*”. The following notations are used: $p_{i,j} = p(x_i, y_j)$, $u_{i,j} = u(x_i - \frac{1}{2}h_{i-1}, y_j)$, $v_{i,j} = v(x_i, y_j - \frac{1}{2}k_{j-1})$.

We employ three-point difference approximations for the second-order derivatives

$$\frac{\partial^2 f}{\partial x^2} \Big|_{i,j} = \frac{2}{h_i + h_{i-1}} \left(\frac{f_{i+1,j} - f_{i,j}}{h_i} - \frac{f_{i,j} - f_{i-1,j}}{h_{i-1}} \right) + O(h_i h_{i-1}), \quad (3.1)$$

$$\frac{\partial^2 f}{\partial y^2} \Big|_{i,j} = \frac{2}{k_j + k_{j-1}} \left(\frac{f_{i,j+1} - f_{i,j}}{k_j} - \frac{f_{i,j} - f_{i,j-1}}{k_{j-1}} \right) + O(k_j k_{j-1}), \quad (3.2)$$

where f stands for u , v or p and h_i, k_j stand for the spacings of the respective grid. The derivatives $\partial p/\partial x$ and $\partial p/\partial y$ are approximated respectively on the u -grid (“ \circ ”) and v -grid (“ $*$ ”), while $\partial u/\partial x$ and $\partial v/\partial y$ are approximated on the main p -grid (“ \bullet ”):

$$\left. \frac{\partial p}{\partial x} \right|_{\circ} = \frac{p_{i,j} - p_{i-1,j}}{h_{i-1}} + O(h_{i-1}^2); \left. \frac{\partial p}{\partial y} \right|_{*} = \frac{p_{i,j} - p_{i,j-1}}{k_{j-1}} + O(k_{j-1}^2). \quad (3.3)$$

$$\left. \frac{\partial u}{\partial x} \right|_{\bullet} = \frac{u_{i+1,j} - u_{i,j}}{h_i^u} + O(h_i h_{i-1}); \left. \frac{\partial v}{\partial y} \right|_{\bullet} = \frac{v_{i,j+1} - v_{i,j}}{k_j^v} + O(k_j k_{j-1}). \quad (3.4)$$

In [8, 9] the scheme proposed by Arakawa [3] for the $\psi - \omega$ formulation for ideal flows was extended to Navier-Stokes equations. A similar idea in primitive variables was proposed in [16] with a special reference to the operator-splitting schemes. It has been elaborated further in [7, 6] and forms the basis of the present work.

$$\begin{aligned} \left(\frac{\partial(u^2)}{\partial x} - \frac{u}{2} \frac{\partial u}{\partial x} \right) \Big|_{\circ} &= \frac{(u_{i+1,j}^n + u_{i,j}^n)u_{i+1,j} - (u_{i,j}^n + u_{i-1,j}^n)u_{i-1,j}}{2(h_i^u + h_{i-1}^u)} + O(h_i^u h_{i-1}^u), \\ \left(\frac{\partial(uv)}{\partial y} - \frac{u}{2} \frac{\partial v}{\partial y} \right) \Big|_{\circ} &= \frac{(v_{i,j+1}^n + v_{i-1,j+1}^n)u_{i,j+1} - (v_{i,j}^n + v_{i-1,j}^n)u_{i,j-1}}{2(k_j + k_{j-1})} + O(k_j k_{j-1}), \\ \left(\frac{\partial(uv)}{\partial x} - \frac{v}{2} \frac{\partial u}{\partial x} \right) \Big|_{*} &= \frac{(u_{i+1,j}^n + u_{i+1,j-1}^n)v_{i+1,j} - (u_{i,j}^n + u_{i,j-1}^n)v_{i-1,j}}{2(h_i + h_{i-1})} + O(h_i h_{i-1}), \\ \left(\frac{\partial(v^2)}{\partial y} - \frac{v}{2} \frac{\partial v}{\partial y} \right) \Big|_{*} &= \frac{(v_{i,j+1}^n + v_{i,j}^n)v_{i,j+1} - (v_{i,j}^n + v_{i,j-1}^n)v_{i,j-1}}{2(k_j^v + k_{j-1}^v)} + O(k_j^v k_{j-1}^v). \end{aligned}$$

for which it is easy to verify the equalities

$$(C_u^h[u], u) = 0, \quad (C_v^h[u], u) = 0, \quad (C_u^h[v], v) = 0, \quad (C_v^h[v], v) = 0.$$

One of the systems for the respective velocity component is always conjugated to the system for pressure set function. For instance, on the first half-time stage one is to solve two linear algebraic systems: one for the difference function

$$\mathbf{v}^{n+\frac{1}{2}} = \text{column}[v_{1,j}^{n+\frac{1}{2}}, \dots, v_{i,j}^{n+\frac{1}{2}}, \dots, v_{N_x,j}^{n+\frac{1}{2}}, v_{N_x+1,j}^{n+\frac{1}{2}}]$$

with tridiagonal matrix, and a conjugated one – for the “composite” difference function

$$\mathbf{w}^{n+\frac{1}{2}} = \text{column}[u_{1,j}^{n+\frac{1}{2}}, p_{1,j}^{n+\frac{1}{2}}, \dots, u_{i,j}^{n+\frac{1}{2}}, p_{i,j}^{n+\frac{1}{2}}, \dots, u_{N_x,j}^{n+\frac{1}{2}}, p_{N_x,j}^{n+\frac{1}{2}}, u_{N_x+1,j}^{n+\frac{1}{2}}]$$

which turns out to be a pentadiagonal system twice the size of the tridiagonal one.

On the second half-time step one has to solve a tridiagonal system for

$$\mathbf{u}^{n+1} = \text{column}[u_{i,1}^{n+1}, \dots, u_{i,j}^{n+1}, \dots, u_{i,N_y}^{n+1}, u_{i,N_y+1}^{n+1}]$$

and a pentadiagonal system for the “composite” difference function

$$\mathbf{z}^{n+1} = \text{column}[v_{i,1}^{n+1}, p_{i,1}^{n+1}, \dots, v_{i,j}^{n+1}, p_{i,j}^{n+1}, \dots, v_{i,N_y}^{n+1}, p_{i,N_y}^{n+1}, v_{i,N_y+1}^{n+1}],$$

We solve the multidagonal systems by means of a specialized Gaussian-elimination solver [5] employing pivoting which is a generalization of what in the tridiagonal case is called Thomas algorithm.

The general sequence of the algorithm is as follows

- (i) Set values of the parameters Re , τ , ε , N_x , N_y and the initial guess $u_{i,j}^0$, $v_{i,j}^0$, $p_{i,j}^0$;
- (ii) Calculate the values $u_{i,j}^{n+\frac{1}{2}}$, $v_{i,j}^{n+\frac{1}{2}}$, $p_{i,j}^{n+\frac{1}{2}}$ assuming $u_{i,j}^n$, $v_{i,j}^n$, $p_{i,j}^n$ to be known;
- (iii) Calculate the values $u_{i,j}^{n+1}$, $v_{i,j}^{n+1}$, $p_{i,j}^{n+1}$ using $u_{i,j}^n$, $v_{i,j}^n$, $p_{i,j}^n$ and $u_{i,j}^{n+\frac{1}{2}}$, $v_{i,j}^{n+\frac{1}{2}}$, $p_{i,j}^{n+\frac{1}{2}}$.
Set the pressure $p_{i,j}^{n+1} := p_{i,j}^{n+1} - \hat{p}^{n+1}$, where \hat{p}^{n+1} is the average of the pressure;
- (iv) If the following criterion is satisfied

$$\max\{R^u(n), R^v(n), R^p(n)\} \leq \varepsilon, \quad \text{where} \quad R^f(n) \stackrel{\text{def}}{=} \frac{\max_{i,j} |f_{i,j}^{n+1} - f_{i,j}^n|}{\tau \max_{i,j} |f_{i,j}^{n+1}|} \quad (3.5)$$

then the calculation are terminated. Otherwise the index of iterations is stepped up $n := n + 1$ and the algorithm is returned to step (ii).

4. Numerical Results. To verify the practical properties of the new scheme we conduct numerical tests with different benchmark problems for large values of Re using fine grids (uniform or not).

First we consider the following two analytic solutions of the Navier-Stokes equations

$$u = \frac{1}{\text{Re}} - \exp(x + y), \quad v = \frac{1}{\text{Re}} + \exp(x + y), \quad p = 0, \quad (4.1)$$

$$u = \exp(y) \cos(x), \quad v = \exp(y) \sin(x), \quad p = -\frac{1}{2} \exp(2y). \quad (4.2)$$

The numerical calculations are conducted in the region $\Omega = \{0 \leq x \leq 1, 0 \leq y \leq 1\}$ on a uniform grid. The first solution depends on Re , while the second one has nonzero pressure gradient. From the analytical expressions (4.1), (4.2) are derived the respective Dirichlet b.c. for velocity components. No boundary condition is imposed on the pressure function. The following maximal and average errors are used:

$$\epsilon_{\max} = \max_{i,j} |f_{i,j}^{\text{num.}} - f_{i,j}^{\text{anal.}}|, \quad \epsilon_{\text{aver}} = \frac{1}{N_x N_y} \sum_{i,j} |f_{i,j}^{\text{num.}} - f_{i,j}^{\text{anal.}}|, \quad (4.3)$$

where f stands for one of the functions u , v or p .

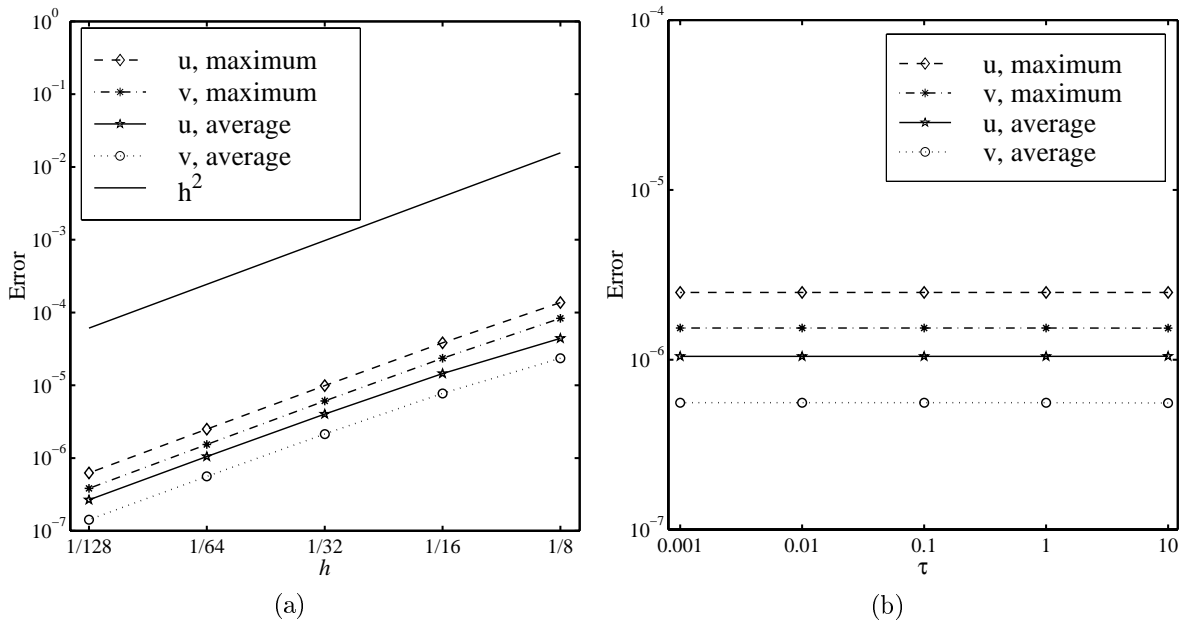


FIG. 4.1. Error in the solution (4.2) for $\text{Re} = 10$ as a function of the: (a) mesh spacing $h = h_x = h_y$, $\tau = 0.1$; (b) time increment τ , $h = 1/32$.

The maximal and average discretization errors for u and v in (4.2) are presented in Figure 4.1 for $\text{Re} = 10$. The left panel shows the error for different grid spacings. It is readily seen that the truncation error is of order $O(h^2)$. In its turn the results presented in Figure 4.1 (b) confirm that there is no dependence of the steady-state solution on the magnitude of time increment τ .

The second featuring example is the well-known lid-driven cavity problem. Lid-driven flow in a square cavity has always been a standard case study for any new scheme for Navier-Stokes equations. Results are available for this flow problem from a number of sources (see [6] for a literature survey). Here we consider a rectangular cavity occupying the region $\Omega = \{0 \leq x \leq a, 0 \leq y \leq b\}$ and the boundary conditions read

$$u(x, 0) = u(0, y) = u(a, y) = 0, \quad u(x, b) = 1, \quad (4.4)$$

$$v(x, 0) = v(x, b) = v(0, y) = v(a, y) = 0 \quad (4.5)$$

$$u_x(0, y) = u_x(a, y) = v_y(x, 0) = v_y(x, b) = 0. \quad (4.6)$$

Alongside with the Reynolds number Re , the aspect ratio $A = b/a$ enters as a second parameter. The flow régime is more complex for deeper cavities. For instance, the results in [12] indicate a Hopf bifurcation for the flow with $A \in [1, 2]$ for $2000 \leq Re_c \leq 10,000$. Steady solutions for $A = 2$ were obtained in [4, 11]. We consider a rectangular cavity with aspect ratio $A = 2$. All computations are done with $\varepsilon = 10^{-10}$ in (3.5).

TABLE 4.1
Coordinates of the extrema of the stream function.

Re	Ref. data	1/h	Primary Top Vortex		Primary Bottom Vortex	
			ψ_{\min}	(x_{\min}, y_{\min})	ψ_{\max}	(x_{\max}, y_{\max})
1000	[4]	256	-0.1169	(0.5273, 1.5625)	0.0148	(0.3516, 0.7891)
	[11]	256	-0.1187	(0.5313, 1.5781)	0.0132	(0.3359, 0.8476)
	Pr.	256	-0.114547	(0.5309, 1.5791)	0.012763	(0.3423, 0.8373)
	Pr.	512	-0.117095	(0.5302, 1.5794)	0.013119	(0.3423, 0.8378)
	Pr.	R256	-0.117945	(0.5299, 1.5795)	0.013330	(0.3424, 0.8379)
3200	Pr.	256	-0.113984	(0.5183, 1.5625)	0.017716	(0.4489, 0.6829)
	Pr.	512	-0.118552	(0.5177, 1.5643)	0.018580	(0.4505, 0.6857)
	Pr.	R256	-0.120075	(0.5175, 1.5648)	0.018869	(0.4510, 0.6866)
5000	Pr.	256	-0.112407	(0.5161, 1.5608)	0.019258	(0.4644, 0.6568)
	Pr.	512	-0.118051	(0.5155, 1.5634)	0.020347	(0.4652, 0.6628)
	Pr.	R256	-0.119933	(0.5153, 1.5642)	0.020712	(0.4655, 0.6646)

R – Richardson extrapolation from solutions 256×512 and 512×1024 ; Pr. – present results.

First we use uniform grids with spacings $h = k = 1/64, 1/128, 1/256, 1/512$. The rate of approaching the steady solution depends on the time increment τ . The optimal value of τ is found from the numerical experiments to be $\tau \approx 0.09$. The final results for a given Reynolds number are obtained as a Richardson extrapolation from the solutions with $h = 1/256$ and $h = 1/512$ and used as benchmark. Different non-uniform grids are used and the results are compared to the benchmark calculations. As a rule, the overall accuracy of the numerical solution obtained with $h = 1/128$ on a uniform grid is the same as the benchmark solution with $h = 1/512$ on the uniform grid.

The streamlines and vorticity isolines are presented in Figure 4.2 for $Re = 1000, 3200$, and 5000 . There is a significant difference between our results [4] in the lower part of the cavity. This is probably due to instabilities during iterations reported in [4]. The bottom-right and bottom-left secondary vortices are more intensive in our work comparing to [11]. The locations and intensities of the primary and the secondary vortex are presented in Table 4.1 for $Re = 1000$. There is a good agreement between our results and [4] for ψ_{\min} , while for ψ_{\max} the computational results in [11] are closer to our results (the difference is less about 1% whereas the difference from [4] is greater than 10%). For Reynolds numbers $Re > 1000$ we unable to find in the literature a steady state solution for comparisons.

Here is due a note on the stability of the method. The distinctive feature of the present implementation is the artificial time which renders the steady-state problem under consideration into Cauchy-Kovalevskaya system. At the time, the physically unsteady Navier Stokes equations are not a system of the said type. For this reason the stability properties of our boundary-value problem can differ from the respective properties of unsteady Navier-Stokes model. It should not surprise that we were able to reach higher Reynolds numbers than in the predominant part of the works available in the literature and that our results are spatially smoother. This is partly due to the fact that we solve a coupled *parabolic* system for velocity components and pressure. The threshold of instability of our calculations cannot be immediately compared to the experiment. The same reasoning applies also to the iterative numerical solutions available from the literature with the difference that the stability properties of those solutions may also differ on their own from the physical stability due to the approximations employed there and the pseudo-time introduced inevitably by any iterative procedure.

5. Conclusions. In the present work a new operator-splitting algorithm is proposed for the incompressible Navier-Stokes equations in primitive variables. On each intermediate half-time step the pressure remains coupled to one of the velocity components and the boundary conditions on velocity components are satisfied strictly without the need to supplement them with artificial conditions for the pressure. The difference scheme employs conservative approximations for the non-linear terms on non-uniform grid. The good agreement between the results obtained here and the known analytical and/or numerical results confirm the properties of the new scheme. The range of Reynolds number for which stationary solutions are obtained exceeds significantly the literature.

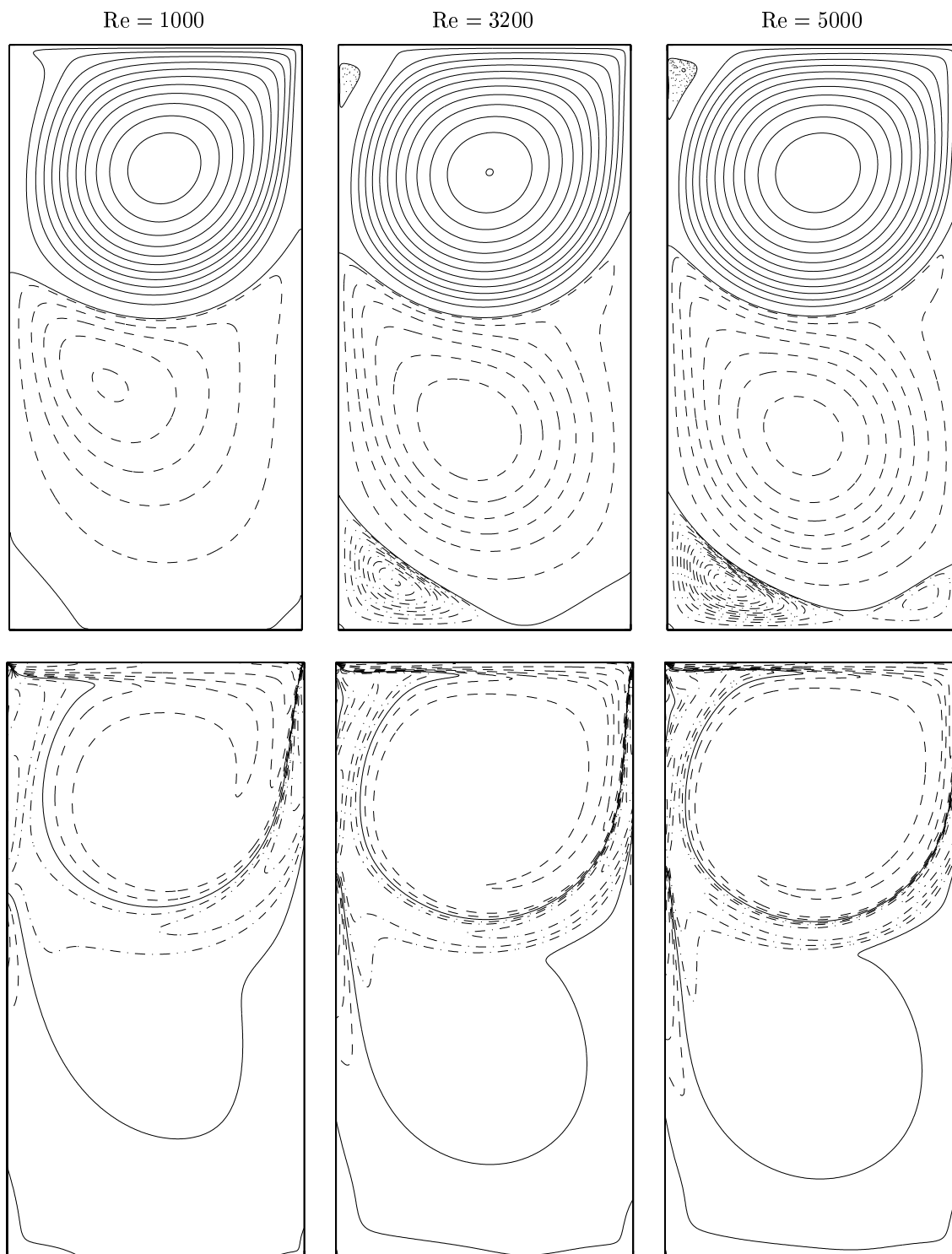


FIG. 4.2. Upper panels: Streamlines for different Reynolds numbers with contour values: — starting from zero with increment -0.01 ; - - - starting from $+0.001$ with increment $+0.003$; - · - · - starting from -0.00002 with increment -0.00004 ; · · · · · starting from $+0.0001$ with increment $+0.0001$. Lower panels: Vorticity isolines with contour values: — 0; - - - $-1, -2, -2^2, -2^3, -2^4$, etc.; - · - · - $1, 2, 2^2, 2^3, 2^4$, etc.

REFERENCES

- [1] S. ABDALLAH, *Numerical solutions for the incompressible Navier-Stokes equations in primitive variables using a non-staggered grid. Part II*, J. Comput. Phys, 70 (1987), pp. 193–202.
- [2] ———, *Numerical solutions for the pressure Poisson equation with Neumann boundary condition using a non-staggered grid. Part I*, J. Comput. Phys, 70 (1987), pp. 182–192.
- [3] A. ARAKAWA, *Computational design for long-term numerical integration of the equations of fluid motion: Two-dimensional incompressible flow. Part I*, J. Comput. Phys., 1 (1966), pp. 119–143.
- [4] C.-H. BRUNEAU AND C. JOURON, *An efficient scheme for solving steady incompressible Navier-Stokes equations*, J. Comput. Phys., 89 (1990), pp. 389–413.
- [5] C. I. CHRISTOV, *Gaussian Elimination with Pivoting for Multitridiagonal Systems, Internal Report 4*, University of Reading, 1994.
- [6] C. I. CHRISTOV AND R. S. MARINOVA, *Implicit vectorial operator splitting for incompressible navier-stokes equations in primitive variables*, Comput. Methods in Applied Mech. Engrn.
- [7] ———, *Implicit scheme for Navier–Stokes equations in primitive variables via vectorial operator splitting*, in Notes on Numer. Fluid Mech., M. Griebel, O. P. Iliev, S. D. Margenov, and P. S. Vassilevski, eds., vol. 62, Wiesbaden, 1998, Vieweg, pp. 251–259.
- [8] C. I. CHRISTOV AND A. RIDHA, *Splitting scheme for iterative solution of bi-harmonic equation. application to 2d Navier–Stokes problems*, in Advances in Numerical Methods and Applications. Proc. of 3rd Int. Conf. on Numerical Methods $O(h^3)$ August 1994, Sofia, Bulgaria, I. Dimov, B. Sendov, and P. Vasilevskii, eds., Singapore, 1994, World Scientific, pp. 341–352.
- [9] ———, *Splitting scheme for the stream-function formulation of 2D unsteady Navier-Stokes equations*, C. R. Acad. Sci. Paris, t. 320, II b (1995), pp. 441–446.
- [10] J. DOUGLAS, *On the numerical integration of $\partial^2 u / \partial x^2 + \partial^2 u / \partial y^2$ by implicit methods*, SIAM Journal, 3 (1955), pp. 42–65.
- [11] O. GOYON, *High-Reynolds number solutions of Navier-Stokes equation using incremental unknowns*, Comput. Meth. Appl. Mech. Engrg., 130 (1996), pp. 319–355.
- [12] K. GUSTAFSON AND K. HALASI, *Cavity flow dynamics at higher Reynolds number and higher aspect ratio*, J. Comput. Phys., 70 (1987), pp. 271–283.
- [13] A. D. HENSHAW, *A fourth-order accurate method for the incompressible Navier-Stokes equations on overlapping grids*, J. Comp. Phys., 113 (1994), pp. 13–35.
- [14] A. D. HENSHAW, H.-O. KREISS, AND L. G. M. REYNA, *A fourth-order accurate difference approximation for the incompressible Navier-Stokes equations*, Comp. Fluids, 23 (1994), pp. 575–593.
- [15] G. D. MALLISON AND G. DE VAHL DAVIS, *The method of false transients for the solution of coupled elliptic equations*, J. Comput. Phys, 12 (1973), pp. 435–461.
- [16] G. I. MARCHUK, *Methods of Numerical Mathematics*, Springer, Berlin, 1982.
- [17] N. N. YANENKO, *Method of Fractional Steps*, Gordon and Breach, 1971.